Experimental investigation of a packed bed thermal energy storage system

2015 J. Phys.: Conf. Ser. 655 012018

(http://iopscience.iop.org/1742-6596/655/1/012018)

Journal of Physics: Conference Series **655** (2015) 012018 doi:10.1088/1742-6596/655/1/012018

Experimental investigation of a packed bed thermal energy storage system

Mario Cascetta[1], Giorgio Cau[1], Pierpaolo Puddu[1], Fabio Serra[2]

[1]Dep. of Mechanical, Chemical and Materials Engineering (DIMCM), University of Cagliari, via Marengo, 2, 09123 - Cagliari, Italy
[2]Solar Concentration Technologies and Hydrogen from RES Laboratory, Sardegna Ricerche - Z.I. Macchiareddu 09010 Uta (CA) - Italy

E-mail: fabio.serra@sardegnaricerche.it

Abstract. In this work experimental investigations on a thermal energy storage system with a solid material as storage media and air as heat transfer fluid will be presented. The experimental test rig, installed at the DIMCM of the University of Cagliari, consists of a carbon steel tank filled with freely poured alumina beads that allows investigations of heat transfer phenomena in packed beds. The aim of this work is to show the influence of the operating conditions and physical parameters on thermocline formation and, in particular, the thermal behaviour of the thermal energy storage for repeated charging and discharging cycles. Better charging efficiency is obtained for lower values of mass flow rate and maximum air temperature and for increasing aspect ratio. A decreasing influence of the metal wall with continuous operation is also highlighted. In conclusion, the analysis focuses on the thermal hysteresis phenomenon, which causes degradation of the thermocline and the reduction of the energy that can be stored by the accumulator as the repeated number of cycles increases.

1. Introduction

Energy storage is assuming a fundamental role in power generation from renewable energy sources owing to their intermittent and non-programmable nature. Energy storage can be effectively used to decouple electricity production and demand, meet random fluctuations in demand and reduce part-load generation in fossil fuel power plants [1, 2].

In particular, thermal energy storage (TES) systems allow storage of heat for later use and are useful in managing the decoupling between the power required by users and that produced by a solar field [3, 4]. Moreover, TES can be used in numerous commercial and industrial applications, often integrated with conventional energy sources to achieve major reliability by reducing peaks of electricity generation, increasing generation capacity and reducing production costs.

There are several methods for storing thermal energy that can be divided into physical and chemical processes [5]. In every type, a sequential process of charge, storage and discharge is present, and this needs to be reversible to recover the energy stored. Physical processes involve sensible heat and latent heat. The former is by far the most common way of TES: the energy is stored as sensible heat of a liquid or solid material and represents the simplest and least expensive form of thermal storage [6]. When the energy is stored in the form of latent heat, a phase change of the storage material occurs [5, 7]. The chemical type of storage exploits the heat of reaction of a reversible reaction; it has not yet been extensively studied but it will become an attractive option at relatively low cost in the

future [6, 8]. Although technologies based on latent heat and chemical energy are considered the most promising, some technological and economic aspects make sensible heat storage superior [9, 10].

The thermal storage system investigated herein consists of a tank filled with solid beads (packed bed) crossed by air used as heat transfer fluid (HTF). In past decades, flow and heat transfer in packed beds, including random and structured packings, were extensively investigated by many researchers [11]. A packed bed with rocks generally represents the most suitable energy storage solution for air-based solar systems, with the aim to provide thermal comfort inside residential buildings [12].

The most common solution for TES section in concentrating solar power (CSP) plants is today represented by two tank systems with thermal oil or molten salts employed as storage medium [3, 4, 7]. To reduce the cost of the TES section, a thermocline system, based on a single-tank packed bed containing a low-cost filling material can be used [13-16]. In thermocline systems, during the charging phase, the hot HTF flowing from the top of the tank gradually heats the filling material before exiting from the bottom of the tank. A high temperature zone, located in the upper part of the tank, is separated from the low temperature one located in the lower part of the tank by a thermal gradient (thermocline) that moves downwards. During the discharging phase, the flow is reversed and the cold HTF is pumped from the bottom of the tank so that the thermocline moves upwards. The use of low-cost filling materials in a single-tank system reduces the cost of the TES section and the volume of HTF required [15, 16].

Beds packed with rocks are particularly suitable in CSP plants when air is used as HTF [17]. Indeed, these systems allow elimination of operating temperature or pressure constraints due to chemical instability of the HTF or solid material or their interaction and elimination of the need for a heat exchanger between the HTF and the storage medium. On the other hand, owing to the lower volumetric heat capacity and thermal conductivity of air compared to thermal oil or molten salts, a higher air mass flow rate and surface area are required, with higher pressure drops and energy losses.

However, owing to the temperature gradient inside the tank, thermocline systems are less efficient than two-tank systems because of the presence of an unexploited zone of the tank and the progressive reduction of the useful energy during continuous operation due to thermal hysteresis [14, 17, 18].

In this work, an experimental study was carried out to explore how operating conditions, such as mass flow rate or maximum HTF temperature, and physical parameters, such as the aspect ratio of the tank, influence the thermocline formation and, in particular, the thermal behavior of the TES in the case of repeated charging and discharging cycles.

2. Experimental setup and instrumentation

The experimental setup built at DIMCM is shown schematically in Figure 1. It consists of an open circuit where, by operating some valves, it is possible to perform single phases and complete cycles of charging and discharging of the thermal storage.

The TES system consists of an insulated steel tank filled with small alumina spheres. The experimental set-up, equipped with a variable speed screw compressor and an electric heater, allows investigation of heat transfer performance of packed beds using air as heat transfer fluid. An inverter allows changing of the compressor speed to modify the delivered flow rate from 255 to 940 m^3/h of free air. The mass flow rate is evaluated by an orifice plate (Q in Figures 1 and 2) with an uncertainty of about 2.5% of the read value. A PID controller allows modulation of the electrical heater mean power and setting of the air flow temperature to the desired value up to 300 °C. Table 1 provides the most relevant data of the rig.

The storage material is made of commercial sintered alumina beads with a diameter in the range 7-9 mm (Al_2O_3 89.5 wt %) freely poured into the tank with a bed void fraction in the range 0.385-0.395. The net volume of the porous bed inside the reservoir is about 0.5 m^3, 0.58 m in diameter and 1.8 m in height. A layer of 100 mm mineral wool covers the carbon steel tank to minimize thermal losses to the outside. Two flow distributors placed at the top and bottom of the reservoir spread the air uniformly in the porous bed. The temperature profile in the storage tank is carefully investigated using nineteen T-type thermocouples placed along the vertical axis 100 mm from each other in a metallic rack as shown

in Figure 3. Five more thermocouples are placed along a radius, with a decreasing distance from each other close to the wall to investigate the influence of the wall on the temperature profile. Two homemade feed-throughs link the sensors to the outside. The external wall temperature is measured by ten K-type thermocouples along the axial direction and by five K-type thermocouples in the circumferential direction at about 600 mm from the top of the bed. The sensors are fastened using a special high-temperature cement. Other thermocouples are used to measure flow temperature at different locations of the plant to handle the valves before starting the charging or discharging phases.

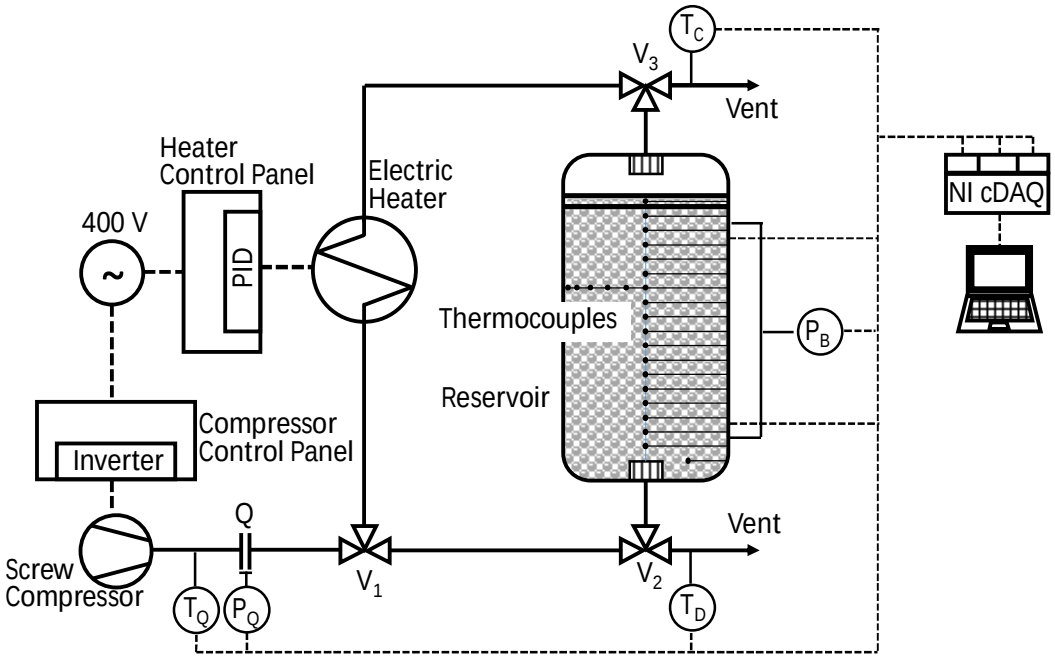

Figure 1. Schematic of the experimental setup.

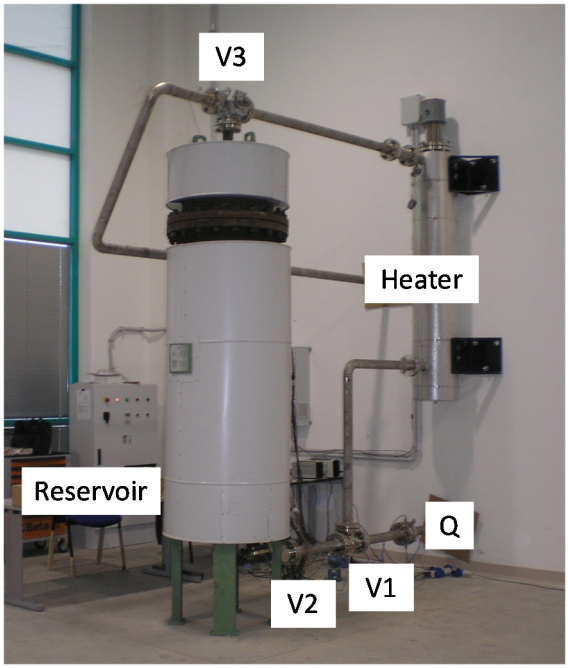

Figure 2. Laboratory test rig.

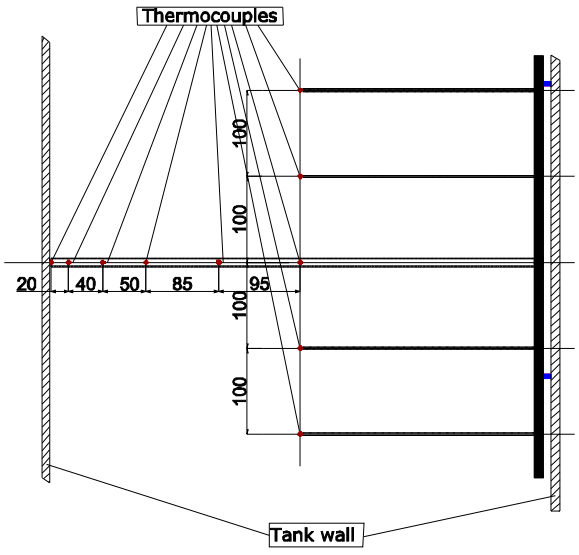

Figure 3. Thermocouple rack.

Table 1. Technical data of rig components.

Compressor delivered flow	255-940 m^3/h, FAD
Electrical heater max. power	70 kW
Maximum air temperature	300 °C
Bed height	1800 mm
Bed diameter	584 mm
Alumina bead diameter	7-9 mm
Alumina bead density	3550 kg/m3
Alumina bead heat capacity (100 °C)	902 J/kgK
Bed void fraction	0.385-0.395
Tank coating thickness (Mineral wool)	100 mm

All the thermocouples are calibrated in the range of 25-300 °C with an uncertainty of ±1°C. A differential pressure transmitter detects the pressure drop along the bed. All signals are acquired by a National Instruments Compact DAQ USB chassis with several modules for thermocouples and analog inputs. The most important recorded signals are monitored with a Graphical User Interface developed using LabVIEW software.

The experimental set-up is suitable for investigating and evaluating performance of the storage system under different operating conditions obtained by varying the mass flow rate, aspect ratio, particle dimension and temperature range during the charging and discharging phases.

Three 3-way stainless steel full-bore valves allow performance of a single phase of charge or discharge as well as repeated sequences of charge and discharge cycles. At the beginning of the first charging phase, the initial temperature of the bed is stabilized sending the air directly from the compressor to the tank. The air flows through valves V1 and V2 from the bottom to the top of the tank before being sent into the atmosphere through valve V3. After this first preliminary phase, the piping connecting the heater to the accumulator is heated until a stable temperature is reached. Subsequently, valve V1 connects the compressor to the heater to allow an increase in air temperature to the desired value, while the air is sent to the vent through valve V3. When the temperature detected by thermocouple TC (Figure 1) reaches the desired value, valve V3 is actuated to start the charging phase. The air moving along the porous bed from the top to the bottom heats the solid material before being vented through V2. During the discharging phase the valves are set as in the preliminary phase to recover the thermal energy stored in the accumulator, sending a flow of cold air from the bottom to the top of the bed. The minimum fluid temperature is determined by the compressor delivery.

3. Experimental characterization and discussion

Defining T_{max} and T_{min} respectively as the maximum and the minimum temperature detected in the porous bed, the temperature distribution can be reported in the dimensionless form (eq. 1):

$$\theta = \frac{T - T_{\min}}{T_{\max} - T_{\min}} \tag{1}$$

Figure 4 (a) depicts the time evolution of the temperature profile along the bed during a typical charge-discharge cycle. During the charging phase, the temperature increases from the top to the bottom of the bed. This phase was stopped when the temperature at the bottom of the tank reached a threshold value given by the tolerance with respect to the minimum temperature allowed by user's needs. Likewise, the discharging phase ended when the temperature at the top of the tank reached a threshold value defined in the same manner with reference to the maximum temperature. In this case a threshold tolerance of about 2.5% (θ=0.025 and 0.975) of the temperature range considered (about 200°C) was assumed. It is possible to observe that the temperature at the top (x/L = 0) changes in time to the maximum value due to the thermal inertia of the upper part of the tank. The discharging phase ended when the temperature at the outlet of the accumulator reached the threshold value. The area between the curves of the temperature distribution at the end of charging and discharging phases is indicative of the useful energy actually recovered during the entire cycle, and shows that most of the

bed is not exploited. The amount of stored energy depends on several process parameters, such as mass flow rate and temperature thresholds, inlet–outlet temperature difference and physical parameters, such as aspect ratio AR (length to diameter ratio L/D), bed void fraction and particles diameter. The influence of some of these parameters will be presented below.

Figure 4 (b) shows the time evolution of the temperature distribution along the radial direction. In about 40% of the radius the temperature falls from an almost constant value to the external wall temperature value. This behavior leads to a further reduction of useful energy. The wall effect along the radius obviously depends strongly on the constructive characteristics of the reservoir and on the working fluid properties, with particular disadvantages for gases with respect to liquids [14, 19].

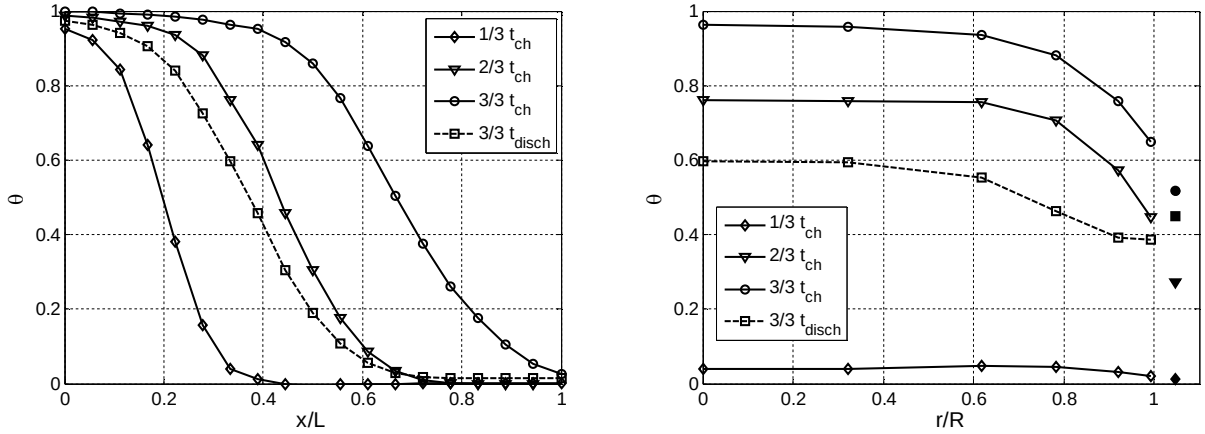

(a) (b)

Figure 4. Temperature distribution during a typical charging-discharging cycle (T_{max} 237°C, T_{min} 38°C, mass flow rate 0.15 kg/s) (a) axial distribution (b) radial distribution (markers placed beyond r/R=1 refers to external wall).

A more effective way to improve the accumulator storage capacity is to increase the threshold tolerance. This solution obviously depends on the value of the temperature threshold that can be accepted by the user. Figure 5 shows a noteworthy increase in the energy stored which is obtained when the outlet dimensionless temperature is equal to 0.2 and 0.3. As shown below, this condition gives benefits also in continuous operation. The same figure reports the effect of mass flow rate on the energy stored in the tank. By reducing the mass flow rate the energy charged increases, and this effect is more evident at lower temperature thresholds. A higher mass flow rate means higher flow velocities, higher convective heat transfer and lower charging time. However, in the case of low mass flow rate the lower velocities determine a lower flux of energy through the bed thus enhancing the release of energy in a smaller portion of the bed, with higher temperature gradients and a steeper temperature profile.

The aspect ratio influence was evaluated by considering three different heights of the bed during a charging phase: L=D (AR=1), L=2D (AR=2) and L=3D (AR=3). Figure 6 shows the temperature distribution along the corresponding heights of the bed during the charging phase, when the threshold values (θ=0.01 and θ=0.2) are reached. A higher aspect ratio leads to higher energy stored with a most significant improvement at lower temperature thresholds. This behavior can be explained by taking into account that the thermal process is characterized by the time constant τ, defined as the ratio between the thermal energy transferred to the storage material and the flux of thermal energy exchanged, i.e. the ratio between the thermal capacity of the storage material and the convective heat transfer of the fluid.

$$\tau = \frac{M_b \cdot c_b}{h_{fb} \cdot A} = \frac{\rho_b \cdot (1-\varepsilon) \cdot L \cdot c_b}{h_{fb}} \tag{2}$$

In eq. 2 M_b, c_b and ρ_b are respectively the mass, the specific heat capacity and the density of the bed, h_{fb} is the heat transfer coefficient between fluid and bed, ε is the bed void fraction, A and L are respectively the cross section area and the length of the bed.

Finally, Figure 7 shows the influence of the inlet temperature on the temperature distribution along the bed during the charging phase. By keeping the minimum temperature constant, a lower inlet temperature allows better exploitation of the bed. The slight difference in the temperature distribution shown in Figure 7 can be justified by considering the variation of the thermal properties of fluid and bed with the temperature.

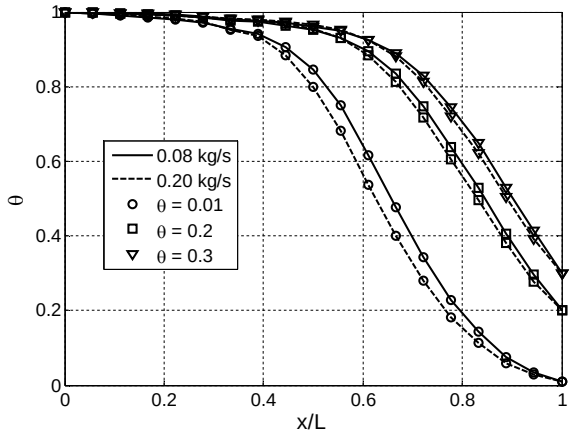

Figure 5. Axial temperature distribution for different mass flow rate and temperature threshold (mass flow rate 0.08 kg/s: T_{max} 230°C, T_{min} 45°C; mass flow rate 0.2 kg/s: T_{max} 239°C, T_{min} 42°C).

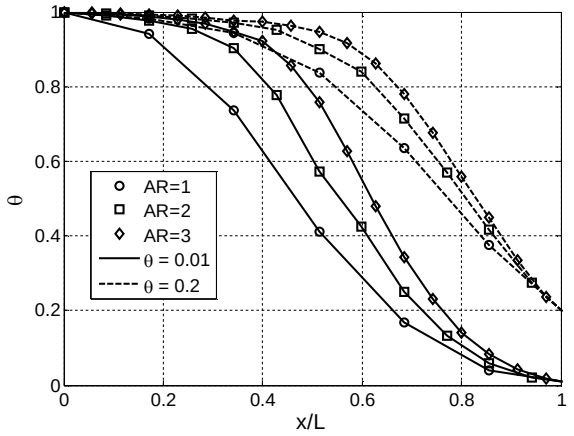

Figure 6. Influence of the aspect ratio on temperature distribution ($T_{max,AR1}$ 226°C (θ=0.01) and 232°C (θ=0.2), $T_{max,AR2}$ 236°C, $T_{max,AR3}$ 239°C, T_{min} 42°C, mass flow rate 0.2 kg/s).

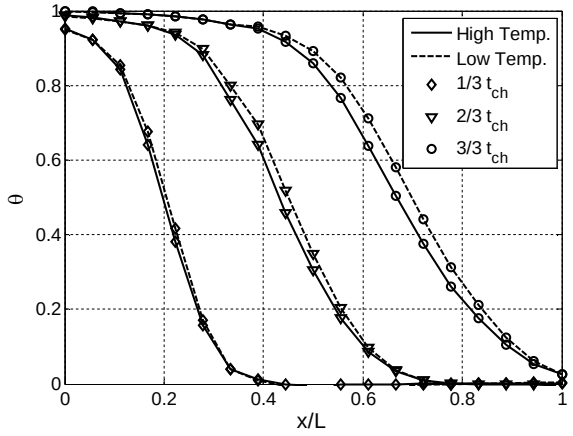

Figure 7. Temperature distribution during the charging phase as a function of the inlet temperature (high temp. T_{max} 237 °C, low temp. T_{max} 158°C, T_{min} 38°C, mass flow rate 0.15 kg/s).

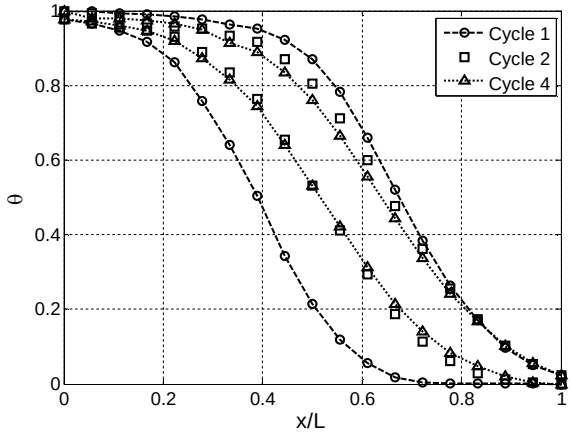

Figure 8. Temperature distribution during continuous operation (T_{max} 191°C, average T_{min} 56°C, threshold tolerance 3°C, mass flow rate 0.2 kg/s).

4. Continuous operation

The TES unit was continuously charged and discharged at a constant mass flow rate. At the beginning of the first charging cycle the temperature along the bed was uniform, while the second cycle started with the temperature profile obtained in the previous phase of discharge. Figure 8 shows the temperature distribution at the end of both charging and discharging phases for four consecutive

cycles. As shown in Figure 8, continuous operation affects TES performance negatively, with a gradual and progressive reduction of the energy that can be stored and recovered. In fact, after four cycles the useful energy is more than halved. Performance improvement of the thermal energy storage system was investigated during continuous operation for different threshold values. Figure 9a reports the temperature distributions at the end of each charging and discharging phase for seven consecutive cycles with a threshold tolerance of 10% (θ=0.1 and 0.9). Also in this case Figure 9a shows the continuous reduction of the energy that can be stored and recovered from the accumulator. It is evident that after seven cycles no appreciable differences in the temperature distribution are recorded and the bed appears to reach a constant behavior, with no more degradation in the energy transfer between the bed and the HTF. For the same experiment Figure 9b shows the temperature distributions in the external tank surface at the end of the charging and discharging phases for the first and last cycle. The temperature profile of the wall appears to follow the one of the bed until it reaches an almost stationary state, with a reduction of its influence during TES operation.

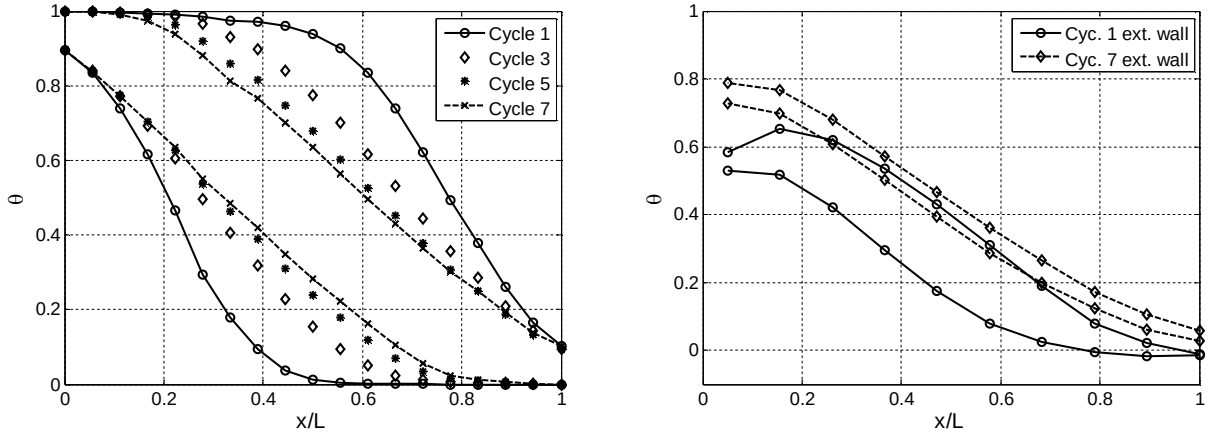

(a) (b)

Figure 9. Temperature evolution during continuous operation with threshold tolerance equals to 10% (θ=0.1 and 0.9) (T_{max} 194°C, average T_{min} 57°C, mass flow rate 0.2 kg/s).

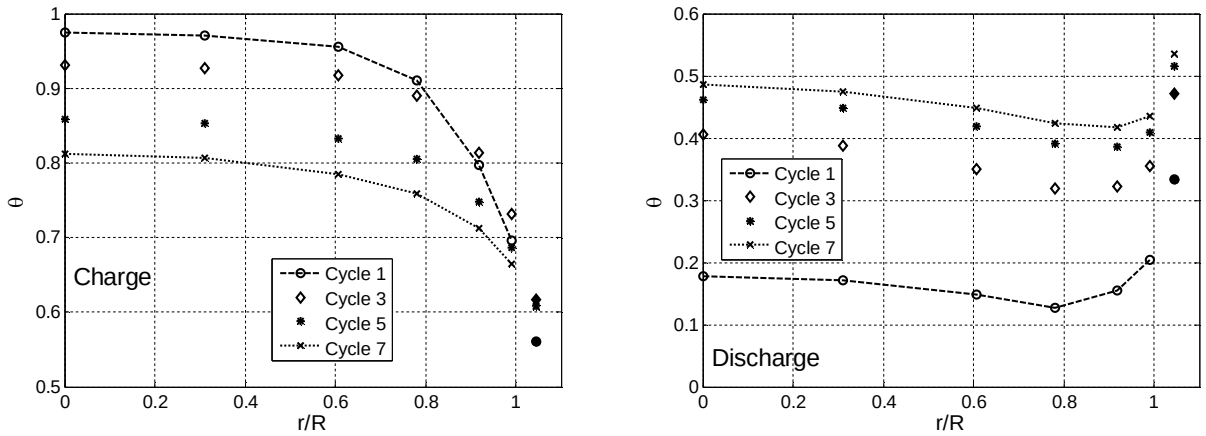

(a) (b)

Figure 10. Radial temperature evolution during continuous operation with threshold tolerance equals to 10% for charging (a) and discharging (b) phase (T_{max} 194°C, average T_{min} 57°C, mass flow rate 0.2 kg/s, markers placed beyond r/R=1 refers to external wall).

Figure 10 depicts how continuous operation affects the radial temperature distribution during the charging and discharging phases. The radial temperature distribution at the end of each charging and

discharging phase during continuous operation shows a progressive decreasing difference between the maximum and minimum temperature along the radius. Moreover the difference in the distribution progressively decreases approaching almost constant behavior as the number of cycles increases (Figures 10a and 10b).

A further improvement can be obtained by increasing the threshold tolerance, as shown in Figure 11a, where a constant behavior seams reached after only four cycles. In this case the reduction of energy stored and recovered during continuous operation is more contained if compared to the previous cases considered. As shown in Figure 10a, also in Figure 11b the radial temperature distribution during the charging phase tends to assume a steady-state value, but with a progressively less marked influence of the wall.

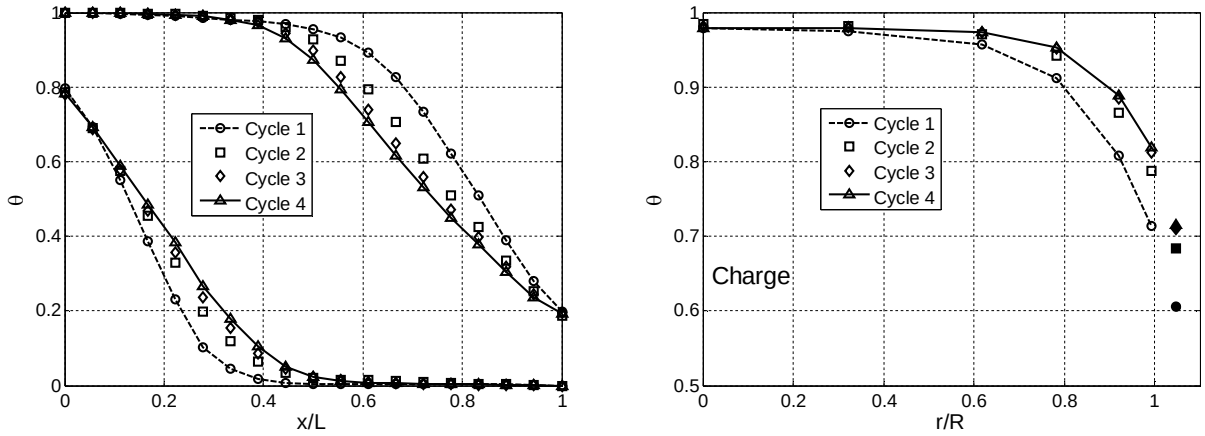

Figure 11. Temperature distribution during continuous operation with threshold tolerance of 20% (θ=0.2 and 0.8) along the vertical axis (a) and the radius (b) (T_{max} 246°C, average T_{min} 56°C, mass flow rate 0.2 kg/s, markers placed beyond r/R=1 refers to external wall).

5. Conclusions

This work presents some results of an experimental investigation on a thermal energy storage system carried out at the Department of Mechanical, Chemical and Materials Engineering of the University of Cagliari. The test facility consists of an open circuit with an insulated steel tank filled with small spheres of alumina, representing the storage media and uses hot air as heat transfer fluid. The influence of some operating conditions and physical characteristics of the system on the formation of the temperature profile "thermocline" was analyzed, as well as the thermal behavior of the TES for repeated cycles of charge and discharge was investigated. The following results from the experimental investigations were obtained:

- energy stored in the bed can be increased increasing the temperature threshold (higher value of the dimensionless temperature θ), the aspect ratio and reducing the mass flow rate;
- slightly higher energy can be stored in the bed if the charging phase is performed at a lower maximum temperature;
- radial temperature distribution shows that metal wall influence cannot be neglected. Radial temperature gradient in observed for at least of 40% of the tank radius from the wall;
- thermal hysteresis is evidenced during repeated cycle operation, highlighting the reducing capacity of the energy stored in the bed (after 4 cycles a reduction of about 60% with a threshold tolerance of 3°C is observed in Figure 8);
- performance of the thermal energy storage system are improved increasing the threshold tolerance between the exit air temperature and the minimum temperature during the charging phases and the maximum gas temperature during the discharging phases.

- a threshold tolerance of 20% of the temperature range considered, shows a considerable improvement of the net useful energy that can be stored after many cycles of continuous operation and a less influence of the thermal hysteresis (only a reduction of about 20% is obtained with a threshold tolerance of 20% in Figure 11).

References

[1] Kousksou T, Bruel P, Jamil A, ElRhafiki T and Zeraouli Y 2014 Energy storage: Applications and challenges *Sol. Energ. Mat. Sol. C.* **120** 59–80
[2] Hadjipaschalis I, Poullikkas A and Efthimiou V 2009 Overview of current and future energy storage technologies for electric power applications *Renew. Sust. Energ. Rev.* **13** 1513–22
[3] Tian Y and Zhao C Y 2013 A review of solar collectors and thermal energy storage in solar thermal applications *Appl. Energ.* **104** 538–53
[4] Medrano M, Gil A, Martorell I, Potau X and Cabeza LF 2010 State of the art on high temperature thermal energy storage for power generation. Part 2–Case Studies *Renew. Sust. Energ. Rev.* **14** 56–72
[5] Mehling H and Cabeza LF 2008 *Heat and cold storage with PCM* (Berlin: Springer)
[6] Pilkington Solar International GmbH 2000 Survey of thermal storage for parabolic trough power plants *National Renewable Energy Laboratory Report*
[7] Gil, Medrano, Martorell, Lazaro, Dolado, Zalba and Cabeza 2010 State of the art on high temperature for power generation. Part 1–Concepts, materials and modellization *Renew. Sust. Energ. Rev.* **14** 31–55
[8] Cot-Gores J, Castell A and Cabeza LF 2012 Thermochemical energy storage and conversion: A-state-of-the-art review of the experimental research under practical conditions *Renew. Sust. Energ. Rev.* **16** 5207–24
[9] Fernandes D, Pitié F, Cáceres G and Baeyens J 2012 Thermal energy storage: How previous findings determine current research priorities *Energy* **39** 246-57
[10] Kuravi S, Trahan J, Goswami DY, Rahman MM and Stefanokos EK 2013 Thermal energy storage technologies and systems for concentrating solar power plants *Prog. Energ. Combust.* **39** 285-19
[11] Singh H, Saini RP, Saini JS and April 2010 A review on packed bed solar energy storage systems *Renew. Sust. Energ. Rev.* **14** 1059–69
[12] Coutier JP and Faber EA 1982 Two applications of a numerical approach of heat transfer process within rock beds *Sol. Energy* **29** 451–62
[13] Yang Z and Garimella SV 2010 Thermal analysis of solar thermal energy storage in a molten-salt thermocline *Sol. Energy* **84**, 974-985
[14] Bruch A, Fourmigué JF and Couturier R 2014 Experimental and numerical investigation of a pilot-scale thermal oil packed bed thermal storage system for CSP power plant *Sol. Energy* **105** 116–25
[15] Kolb GJ 2011 Evaluation of annual performance of 2-tank and thermocline thermal storage systems for trough plants *J. Sol. Energ. – T. Asme* **133**
[16] Cocco D and Serra F 2015 Performance comparison of two-tank direct and thermocline thermal energy storage systems for 1 MWe class concentrating solar power plants *Energy* **81** 526-36
[17] Hänchen M, Brückner S and Steinfeld A 2011 High-temperature thermal storage using a packed bed of rocks and heat transfer analysis and experimental validation *Appl. Therm. Eng.* **31** 1798-06
[18] Cascetta M, Cau G, Puddu P and Serra F 2014 Numerical Investigation of a Packed Bed Thermal Energy Storage System with Different Heat Transfer Fluids *Energy Procedia* **45** 598-07
[19] Wen D and Ding Y 2006 Heat transfer of gas flow through a packed bed *Chem. Eng. Sci.* **61** 3532-42